Bioorganic Chemistry 83 (2019) 424–431

Contents lists available at ScienceDirect

Bioorganic Chemistry

journal homepage: www.elsevier.com/locate/bioorg

Synthesis of *N*-benzyl substituted 1,4-imino-L-lyxitols with a basic functional group as selective inhibitors of Golgi α-mannosidase IIb

Tomáš Klunda, Sergej Šesták, Juraj Kóňa, Monika Poláková*

Institute of Chemistry, Center for Glycomics, Slovak Academy of Sciences, Dúbravska cesta 9, SK-845 38 Bratislava, Slovakia

ARTICLE INFO

Keywords:
Pyrrolidine
Golgi mannosidase II
Selectivity
Glycosidase inhibitor
Molecular docking

ABSTRACT

Inhibition of the biosynthesis of complex *N*-glycans in the Golgi apparatus is one of alternative ways to suppress growth of tumor tissue. Eight *N*-benzyl substituted 1,4-imino-L-lyxitols with basic functional groups (amine, amidine, guanidine), hydroxyl and fluoro groups were prepared, optimized their syntheses and tested for their ability to inhibit several α-mannosides from the GH family 38 (GMIIb, LManII and JBMan) as models for human Golgi and lysosomal α-mannoside II. All compounds were found to be selective inhibitors of GMIIb. The most potent structure bearing guanidine group, inhibited GMIIb at the micromolar level (K_i = 19 ± 2 μM) while no significant inhibition (> 2 mM) of LManII and JBMan was observed. Based on molecular docking and pK_a calculations this structure may form two salt bridges with aspartate dyad of the target enzyme improving its inhibitory potency compared with other *N*-benzyl substituted derivatives published in this and previous studies.

1. Introduction

Iminosugars are naturally occurring mimics of glycosides that are able to inhibit various enzymes of medicinal interest, such as glycosyltransferases and glycoside hydrolases [1]. Glycoprocessing enzymes are an interesting therapeutic target because they are responsible for the metabolism of complex carbohydrate structures involved in many biochemical recognition processes. The iminosugars therefore have attracted attention as lead candidates for a treatment of variety of diseases [1–7]. The iminosugars have the ring oxygen replaced with nitrogen which can be protonated under physiological pH. The protonation of the amine is an important factor for inhibition properties of these glycoside mimics and their biological activity is often attributed to protonated iminosugars that structurally resembles oxocarbenium ion-like transition states that are anticipated during enzymatic hydrolysis and synthesis of carbohydrates [8].

The most common naturally occurring iminosugars possess a polyhydroxylated pyrrolidine core that can be additionally annulated as in pyrrolizidines and indolizidines. Synthesis of both naturally occurring iminosugars and their analogs provides a wide variety of structures and substituents that give the compounds with different ability to inhibit glycoprocessing enzymes [9,10]. The synthesis of various derivatives having pyrrolidine core as interesting bioactive compounds is well documented [11,12]. Many of them exhibited an inhibitory activity against a wide range of glycosidases. For example, compounds having polyhydroxypyrrolidine cores were found to be potent inhibitors of α-mannosidase [13], α-L-fucosidase [14], α-L-rhamnosidase [14–16], α-glucosidase [17], human β-glucocerebrosidase [18] and β-glucosidase [19]. These studies demonstrated a strong stereochemical impact on potency of glycosidase inhibitors. The stereochemical factors are exemplified by the absence or presence and stereochemistry of hydroxymethyl function, and stereochemistry of hydroxy groups attached to the pyrrolidine unit. In particular, substituents at the positions C-1 and C-5 of the iminosugar are often the key determinants of inhibitory potency and selectivity.

Natural alkaloid swainsonine [(1S,2R,8R,8aR)-trihydroxy-indolizidine] [20] is known as a potent and selective inhibitor of glycoside hydrolases from the GH family 38 [21,22]. The effect of swainsonine on oligosaccharide processing was also elucidated [23]. It binds reversibly to the active site of Golgi α-mannosidase II (GMII) (EC 3.2.1.114) [24] and thus modulates *N*-glycoprotein processing resulting in an accumulation of hybrid type of *N*-glycans [25,26]. The inhibition of *N*-glycan trimming in Golgi apparatus affects tumor growth and metastasis. Therefore, swainsonine has attracted attention as a potential anticancer agent [23,27,28]. It was also well tolerated in clinical trials of short duration [23,29,30]. However, swainsonine and all other known GH38 α-mannosidase inhibitors exhibit also a serious side effect. i.e. they also inhibit broad-specificity GH 38 lysosomal α-mannosidase (LMan) (EC 3.2.1.24) [31,32]. This limits their use as therapeutics due to an accumulation of mannose-containing

* Corresponding author.
E-mail address: chemonca@savba.sk (M. Poláková).

https://doi.org/10.1016/j.bioorg.2018.10.066
Received 21 June 2018; Received in revised form 23 October 2018; Accepted 29 October 2018
Available online 31 October 2018
0045-2068/

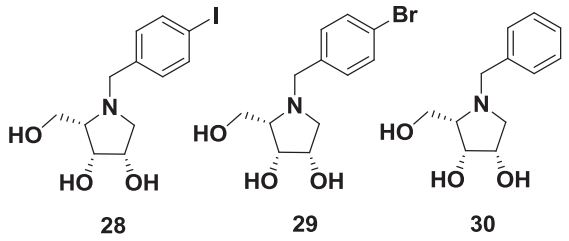

Fig. 1. Structures of the pyrrolidines published by Šesták et al. [37]

oligosaccharides in tissues and serum, and their appearance in urine [23,33].

A series of our previously published articles on synthesis and evaluation of mannosides [34–36] and polyhydroxylated pyrrolidine derivatives [37] led to a finding of the structural features required for a selective GMII inhibitor. Evaluation on a model system of GMIIb enzyme (fruit fly Golgi α-mannosidase II) [38] has shown that such an inhibitor should comprise of a linker of benzyl type and specific stereoconfiguration of hydroxyl and hydroxymethyl functional groups at the saccharide core. Structural design of a lead inhibitor structure, *N*-benzyl 1,4-imino-L-lyxitol (**30** in Fig. 1), was further developed and focused on the modification of the functional group at the position 4 on the benzyl linker. The present paper reports a study of inhibitory properties of eight novel *N*-benzyl substituted pyrrolidines on the GMIIb model system. Most of the derivatives synthesized in this work would bear, at *in vivo* conditions, positive charge on a nitrogen atom of the aminobenzyl moiety. In this way, the binding to the active site of GMII could be improved by forming salt bridges with active-site ionizable amino acids (such as Asp270 and Asp340 in case of GMII [24,39,40], or Asp359 and Glu504 in the model system GMIIb) as it is discussed in this work based on results from molecular modeling.

2. Results and discussion

2.1. Chemistry

The synthesis of target 1,4-imino-L-lyxitols started from either dimesyl derivative **2** or amine **3** (Scheme 1). For both, optimized large scale synthesis started from D-ribose **1** has been published in our previous paper [37].

The cyclization of dimesylate **2** in neat *p*-xylylenediamine was conducted at 95 °C for 16 h and provided 4-(aminomethyl)benzyl derivative **4** which was transformed to the corresponding polyhydroxypyrrolidine **5** by a one-step removal of silyl and isopropylidene groups under acidic conditions (6 M HCl/MeOH) in moderate overall yield.

Primary amine **4** was also an intermediate used for coupling with [*N*,*N*′-bis(*tert*-butoxycarbonyl)]-1*H*-pyrazole-1-carboxamidine [41] with the aim to introduce guanidine function (Scheme 2). The reaction proceeded slowly under conventional heating (50 °C/5 h). Ultrasound irradiation of the reaction resulted in a significant improvement of the reaction yield in shorter reaction time (50 °C/1 h /85%, TLC analysis). Subsequent deprotection of the crude product gave pyrrolidine **6** isolated as hydrochloride in 77% yield (over 2 steps from **4**).

A synthesis of all other compounds commenced from amine **3**. The target pyrrolidine **9** with 4-amidinobenzyl function was prepared in 3 steps in a high overall yield (Scheme 3). *N*-Alkylation of **3** with 4-

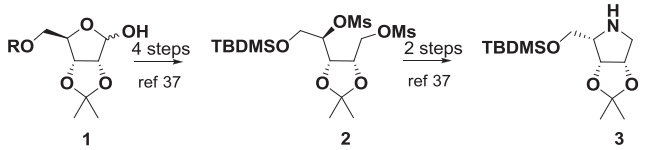

Scheme 1. Synthesis of the intermediates **2** and **3**.

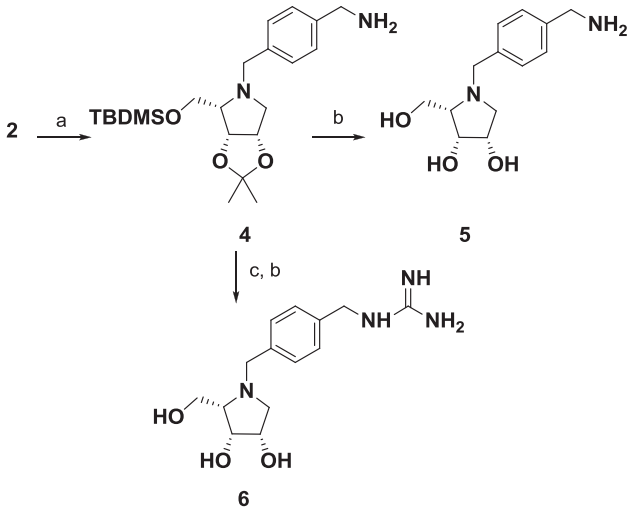

Scheme 2. Synthesis of the pyrrolidines **5** and **6**. *Reagents and conditions*: (a) p-xylylenediamine, 95 °C, 16 h, 63%; (b) [*N*,*N*′-bis(*tert*-butoxycarbonyl)]-1*H*-pyrazole-1-carboxamidine, 50 °C, 1 h, sonication; (c) 6 M HCl/MeOH 1:2 (v/v), rt, 16 h, **5** (78%), **6** (77% in 2 steps).

cyanobenzyl bromide gave **7** almost quantitatively. Conversion of its nitrile function to amidine with LiHMDS in Et_2O proceeded slowly (20% yield of the product after 5 days at room temperature along with some side products as detected by TLC). Interestingly, ultrasound irradiation significantly enhanced the reaction rate. A complete conversion of the starting material to the desired amidine derivative **8** was achieved after 1 h at room temperature. One-step removal of all protective groups afforded *N*-4-amidinobenzyl pyrrolidine **9** as hydrochloride.

Another compound of this series was *N*-4-(2-aminoethyl)benzyl pyrrolidine **14** having one carbon longer alkylamino chain at the position 4 of the benzyl moiety than **5** (Scheme 4). 2-(4-Bromomethylphenyl)-acetamide **10** [42] was synthesized from the corresponding acid in two steps ($SOCl_2/NH_3$) in an improved yield (84% in comparison with 63% [42]) and was fully characterized by ^1H and ^{13}C NMR data. Alkylation of **3** with **10** afforded ***N***-substituted pyrrolidine **11** which was converted to nitrile derivative **12** by dehydration of amide group ($(CF_3CO_2)O$/py) at low temperature. Subsequent transformation of **12** to amine was achieved by reduction with $LiEt_3BH$. A yield of the desired *N*-4-(2-aminoethyl)benzyl pyrrolidine **13** under conventional conditions was not satisfactory ($LiEt_3BH$, THF, 0 °C, 4 h, 38%). The reduction was therefore examined to be carried out under ultrasound irradiation. In this way, the nitrile function of **12** was converted to the amine **13** much faster (45 min) in a good yield (69%). The target pyrrolidine **14** was obtained after acidic deprotection.

A synthesis of the 4-(silyloxy)benzyl bromide **17** is depicted in Scheme 5. Silylation of *p*-cresol gave the silyl ether **16** [43] in a quantitative yield. Its bromination under slightly modified conditions, previously applied for synthesis of a very similar *p*-cresol derivative [44], afforded the required bromide **17**. The modification consisted in an application of chloroform and NBS/AIBN/ultrasound irradiation at 66 °C instead of CCl_4 and benzoylperoxide/UV at 80 °C, led to a faster conversion and almost quantitative yield of the product **17**, which was used directly in the next step.

For a synthesis of the pyrrolidines **18**, **20**, **22** and **23**, amine **3** was combined with the corresponding bromides (Scheme 6). Reduction of the nitrobenzyl derivatives **18** and **20** with $SnCl_2$ in EtOH at a higher temperature (70 °C) provided aminobenzyl counterparts in low yields (10–25%). An application of the same reduction conditions under ultrasound irradiation led to a significant increase in the amines yield (69–83%). Alkylation of **3** with 4-fluorobenzyl bromide or **17** yielded **22** and **23**, respectively. Finally, one-step deprotection of **19** and **21**–**23**

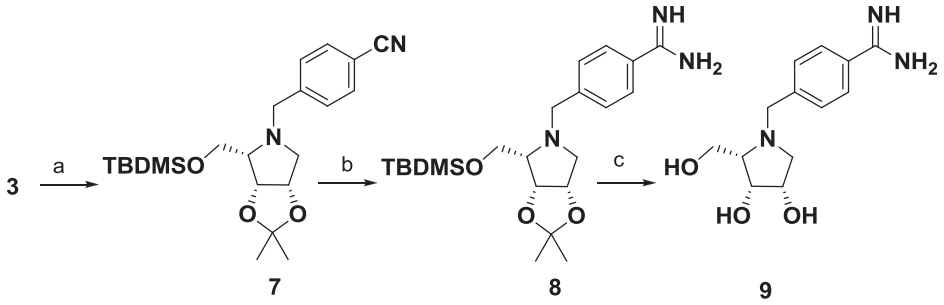

Scheme 3. Synthesis of the pyrrolidine **9**. *Reagents and conditions*: (a) 4-CN BnBr, K_2CO_3, DMF, 40 °C, 3 h, 99%; (b) LiHMDS, Et_2O, rt, 1 h, sonication, 95%; (c) 6 M HCl/MeOH 1:2 (v/v), rt, 16 h, 84%.

afforded the polyhydroxypyrrolidines **24–27**.

In summary, a series of *N*-benzyl polyhydroxypyrrolidines having various substituents at the benzyl moiety was prepared. The presence of these groups with a different size and chemical properties is important to study the interactions between the inhibitor and the active site of an enzyme (for more details see the Section 2.3. *Molecular modeling*).

Sonication was successfully applied in some steps of the synthesis to facilitate or improve the reaction rate and conversion to desired products. This demonstrated that ultrasound irradiation [45] is an alternative and efficient tool to get some compounds, which are otherwise hardly obtained or prepared in an unsatisfactory yield under conventional conditions.

2.2. Enzyme assay

Eight *N*-benzyl substituted 1,4-imino-L-lyxitols **5**, **6**, **9**, **14**, **24–27** were evaluated against the class II α-mannosidases GMIIb (a model of Golgi α-mannosidase II from a fruit fly) [38], LManII (a model of lysosomal α-mannosidase from a fruit fly) [38] and JBMan (Jack bean α-mannosidase, the plant homologue of the acidic class II mannosidases) [46] from the GH38 family to investigate their ability to selectively inhibit only the enzyme from Golgi apparatus. All tested pyrrolidines selectively inhibited the target enzyme GMIIb with IC_{50} values in a range from 42 µM to 155 µM. No significant inhibition of LManII (or JBMan) was observed.

The pyrrolidines **5**, **6**, **9**, **14**, **24** and **25** have at the benzyl unit a functional group (amine, amidine or guanidine) which can be protonated at the physiological pH (for more details see a discussion in the Section 2.3. *Molecular modeling*). Among them, the compound **9** with amidine function (IC_{50} = 155 µM) was found to be the weakest GMIIb inhibitor. The presence of amino function directly attached to the

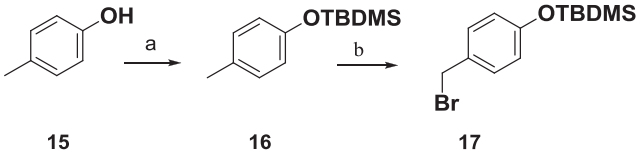

Scheme 5. Synthesis of the bromide **17**. *Reagents and conditions*: (a) TBDMSCl, imidazole, DMF, rt, 16 h, 99%; (b) NBS, AIBN, $CHCl_3$, 66 °C, 40 min, sonication, 99%.

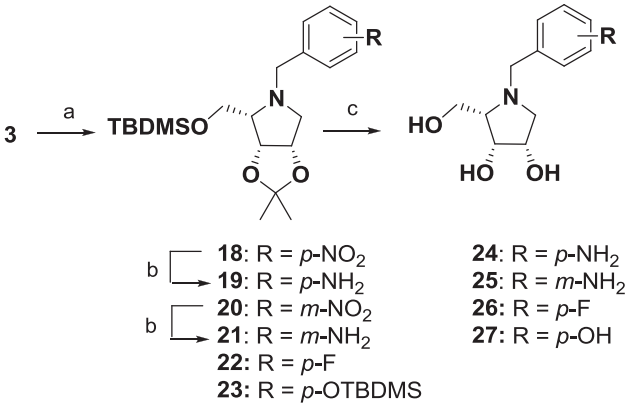

Scheme 6. Synthesis of the pyrrolidines **24–27**. *Reagents and conditions*: (a) RBr, K_2CO_3, DMF, 40 °C, 3 h, **18** (94%), **20** (96%), **22** (92%), **23** (63%); (b) $SnCl_2$, EtOH, 70 °C, 30 min, sonication, **19** (69%), **21** (83%); (c) 6 M HCl/MeOH 1:2 (v/v), rt, 16 h, **24** (82%), **25** (87%), **26** (64%), **27** (70%).

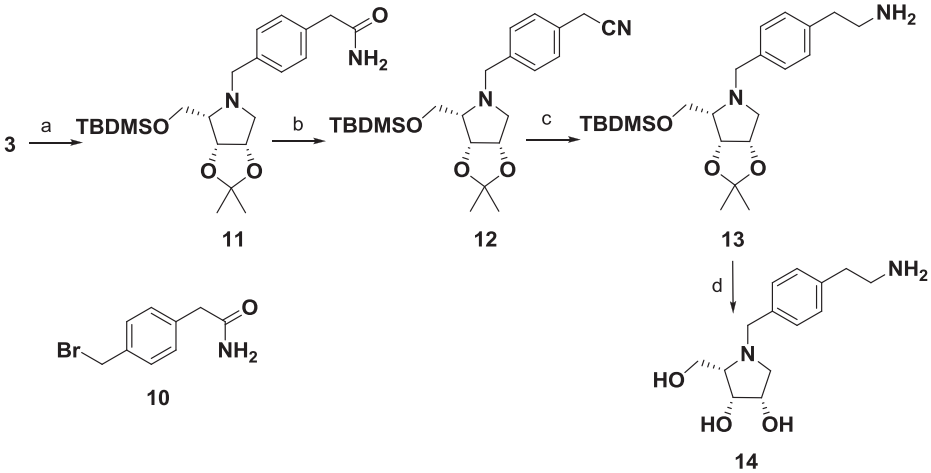

Scheme 4. Synthesis of the pyrrolidine **14**. *Reagents and conditions*: (a) **10**, K_2CO_3, DMF, 40 °C, 3 h, 98%; (b) $(CF_3CO)_2O$, pyridine, −35 °C, 2 h, 99%; (c) $LiEt_3BH$, THF, 0–5 °C, 45 min, sonication, 69%; (d) 6 M HCl/MeOH 1:2 (v/v), rt, 16 h, 75%.

Table 1
Inhibition of class II GH38 α-mannosidases (GMIIb, LManII and JBMan) by various *N*-benzyl substituted 1,4-imino-L-lyxitols.

	IC_{50} (K_i) in μM		
Compound	**GMIIb**	**LManII**[a]	**JBMan**[a]
5	115 ± 18	n.i.	n.i.
6	42 ± 12 (19 ± 2)	n.i.	n.i.
9	155 ± 28	n.i.	n.i.
14	120 ± 22	n.i.	n.i.
24	125 ± 15	n.i.	n.i.
25	142 ± 16	n.i.	n.i.
26	129 ± 11	n.i.	n.i.
27	152 ± 25	n.i.	n.i.
28	52 ± 12 (50 ± 12)[b]	6100[b]	n.i.[b,c]
29	55 ± 15 (58 ± 6)[b]	7500[b]	n.i.[b,c]
30	88 ± 0.06 (76 ± 0.13)[b]	2700[b]	n.i.[b,c]

[a] n.i. – no inhibition or inhibition < 10% at 2 mM.
[b] IC_{50} and K_i values measured by Šesták et al. [37].
[c] no inhibition or inhibition < 10% at 2 mM measured by Šesták et al. [37].

benzyl unit led to a slight improvement in their inhibitory activity (IC_{50} values of the compounds **24** and **25** was 125 μM and 142 μM, respectively). Attachment of primary amino function at the benzyl moiety linked through a longer methyl or ethyl chain in the pyrrolidines **5** and **14** resulted in mild increase in their potency, however, regardless the length of the aliphatic linker, the latter compounds had almost the same activity (IC_{50} = 115 μM and 120 μM, respectively).

On the other hand, introduction of guanidine function resulted in the pyrrolidine **6** as the most potent GMIIb inhibitor in this series. Its IC_{50} value of 42 μM was three times lower than that of its precursor **5**, which was the most potent among the pyrrolidines having amine function. The inhibition constant K_i for **6** was 19 μM. Based on K_i values, derivative **6** was an approximately three times more potent GMIIb inhibitor than *p*-I and *p*-Br benzyl pyrrolidines **28** and **29** (Fig. 1 and Table 1) published in our previous study [37].

To understand better the potency of **28** and **29**, *p*-F and *p*-OH benzyl substituted pyrrolidines **26** and **27** were synthesized. However, both were less potent inhibitors of the target GMIIb enzyme (IC_{50} = 129 and 152 μM) and their inhibitory properties weakened in the following order: *p*-I ≈ *p*-Br > *p*-F > *p*-OH.

An important requirement on a GMII inhibitor is its selective inhibition of only Golgi α-mannosidase, with reduced activity toward lysosomal mannosidases. All tested 1,4-imino-L-lyxitols exhibited negligible efficiency toward LManII. The compounds were also tested with another GH38 enzyme, α-mannosidase from *Canavalia ensiformis* (JBMan, EC 3.2.1.24) which is widely used as a model for acidic α-mannosidases [35–37,47,48]. JBMan was inhibited very weakly by all pyrrolidines (1–8% inhibition of JBMan at the 2 mM concentration of the inhibitors).

In summary, the potency and selectivity of the pyrrolidines **5**, **6**, **9**, **14**, **24** and **25** with ionizable functional groups, in particular the most potent compound **6**, is similar to *p*-halobenzyl pyrrolidines **28** and **29**, which were previously shown [37] to exhibit the best activity against the target enzyme GMIIb. This study demonstrates that the presence of ionizable NH_2 function at the benzyl unit of the inhibitor had a certain impact on potency and binding of the inhibitor to the active site of distinct GH38 enzymes. Thus, an identification of the structure of appropriate substituent at the benzyl moiety may be a way for improvement of the selectivity of the GMIIb inhibitor.

2.3. Molecular modeling

A series of *N*-benzyl substituted 1,4-imino-L-lyxitols with amine, amidine and guanidine groups were proposed based on molecular docking as new candidates for selective GMII inhibitors. The design was based on our previous work [35] in which a possible next inhibitor binding subsite in dGMII, consisted of the dyad Asp340-Asp270, was tested in this study. A Schrödinger library of small fragments, derived from molecules in the medicinal chemistry literature, was docked into both target enzyme (dGMII) and the enzyme model for the unwanted co-inhibition (bLMan). The fragments were docked around the dyad Asp340-Asp270 (dGMII) and the dyad Ser318-Asn262 (bLMan) to design "a prolonged arm" of a selective GMII inhibitor. The amidine and guanidine fragments provided best scoring for the target enzyme and suitable geometry to connect them to *N*-benzyl polyhydroxypyrrolidine core of the inhibitor. Based on these results, guanidine (**6**) and amine (**14**) derivatives were designed and synthesized. Other amine and amidine derivatives (**24**, **25**, **5** and **9**) were also synthesized as possible alternative structures to the proposed guanidine derivative. Firstly, the synthesized structures were docked into the active site of dGMII, for which a crystal structure is available. Then, the structures were also docked into GMIIb, for which enzymatic assays were measured. The binding modes of the docked inhibitors were similarly predicted, thus, only results of the most potent GMIIb inhibitor **6** of the series will be described and discussed. As it can be seen in Fig. 2, key contacts between the docked inhibitor and the enzyme were found with amino acid residues from a catalytic subsite (i.e. Asp 92, Asp204, Asp341, Asp472, Trp95 and Zn^{2+} ion in dGMII) and an another part of the active site consisted of Arg228, Arg876, Asp340 and Asp270.

The interaction pattern of the pyrrolidine inhibitors with the catalytic subsite of dGMII is analogous with those found in crystal structures with nanomolar inhibitor swainsonine [47,49] and other known inhibitors [39,48,50–55]. The more potent inhibitors have showed to be ones with a longer aminoalkyl or guanidine chains, as **5**, **14** or **6**. These structures seem to have tendency better to interact with Asp340-Asp270 by means of a salt bridge compared with the inhibitors with the shorter chain (**24**, **25** or **9**). For example, distance between carbonyl oxygen of Asp270 and a hydrogen atom of ammonium group of the inhibitor **14** was 2.01 Å, while in **24** it was 3.51 Å. The length of guanidine group attached at the position 4 at the benzyl group of **6** is fitted best for interactions with the dyad Asp340-Asp270 where two salt bridges were indicated from the docking calculations (Fig. 2). Indeed, IC_{50} = 42 μM (K_i = 19 μM) of **6** was 3–5 times better compared with other structures. According to pK_a calculations (discussed in the next section *pK_a calculations*) the guanidine prefers protonated guanidinium form, thus, it could interact with the dyad Asp340-Asp270 by strong salt bridges. This interaction may be less significant for derivatives with a shorter alkyl chain between benzyl and guanidine (or amine) moieties of the inhibitor. It should be noted that in bLMan (the enzyme model for the unwanted co-inhibition) Asp340-Asp270 is substituted by the less polar Ser318-Asn262 dyad and the salt bridges between the guanidine moiety of the inhibitor and enzyme cannot be formed.

Because of enzyme assays were performed with the model enzyme GMIIb [38], all inhibitors were also re-docked into GMIIb (a homology model) to validate conclusions and docking results with dGMII (crystal structure) [47,49]. In the case of GMIIb, docked inhibitors with longer guanidine (or amine) chain preferred interaction with the Asp359-Glu504 dyad, while the shorter ones were not sufficiently close to it to have a significant interaction. This again correlates well with the measured IC_{50} values of the tested compounds. However, it has to be noted that the position of Asp359-Glu504 in GMIIb does not correspond with the above-mentioned Asp341-Asp270 in dGMII, and their positions in overlay are shifted to Tyr267 of dGMII (Fig. 2). Thus, the inhibition assays with fruit fly GMIIb will have to be also validate with human GMII or a homologue of mammalian GMII in future.

pK_a calculations. It is known that pK_a values of amino groups in iminosugars may differ from typical values for amines [22,56]. Most structures synthesized in this study contains two ionizable groups, one in the pyrrolidine ring and the other on the benzene ring. As it was proposed in our previous work [37] different protonation forms of

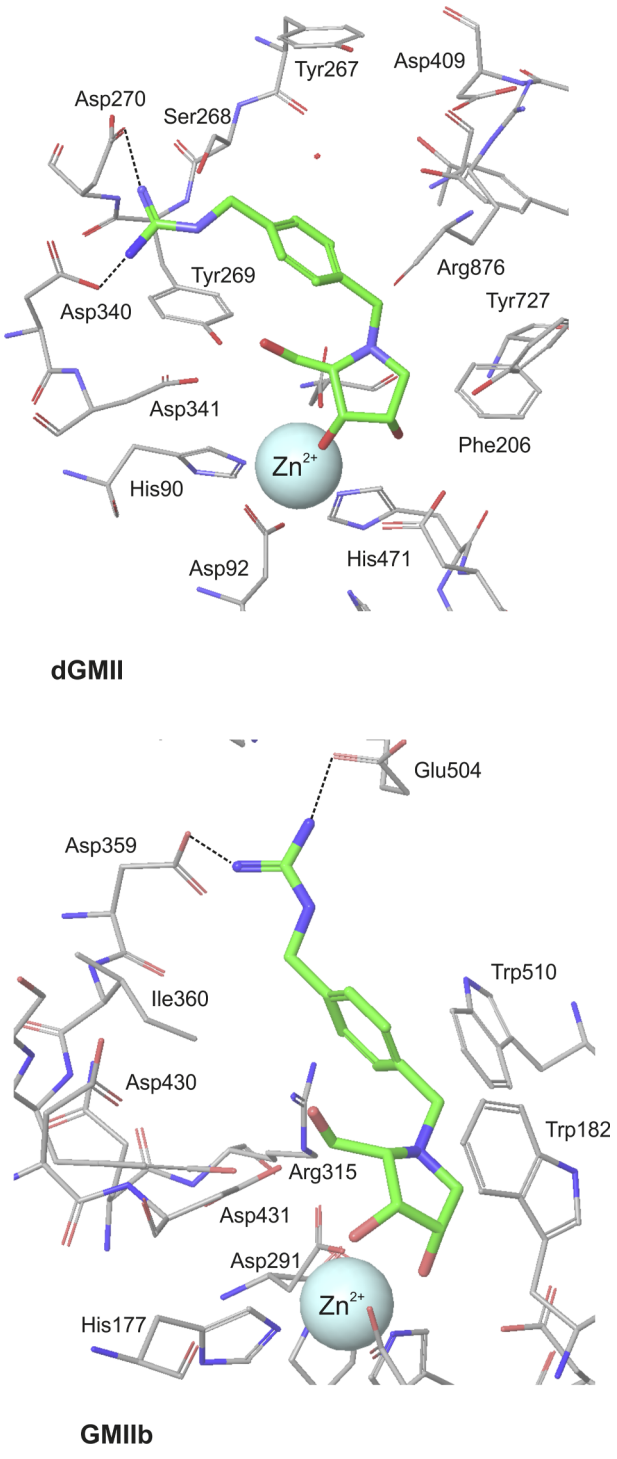

Fig. 2. The structure **6** docked into the active-site of dGMII (PDB ID: 3BLB) [47,49] and GMIIb (homology model). In both cases **6** interacts with its guanidine moiety with a polar dyad (Asp270-Asp340 in dGMII and Asp359-Glu504 in GMIIb). For sake of clarity, hydrogen atoms and some amino acid residues are omitted.

ionizable groups at the inhibitors or the active-site amino acids of the enzyme may influence specific binding and preference toward the target enzyme. Therefore, pK_a values of ionizable groups in the inhibitors in water were calculated and compared with derivatives and known GMII inhibitors calculated in previous studies [37,57]. The results are compiled in Table 2. In all structures except for **24** and **25**, the functional groups with nitrogen prefer protonation forms in pH = 7. In **24** and **25** the amine group attached directly to the benzene ring prefers

Table 2
Calculated pK_a values in water for ionizable groups of the synthesized structures as well as of known GMII inhibitors, swainsonine (SWA) and 1,4-dideoxy-1,4-imino-D-mannitol (DIM).

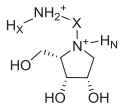

pK_a in water (pH = 7)

Compound	H_N	H_X
26	7.8	
27	7.7	
24	7.2	1.8
25	8.1	1.8
5	7.6	7.2
14	7.5	7.9
9	6.5	9.9
6	7.7	10.1
30	6.3 [a]	
SWA	7.8 [b] (7.5)[c]	
DIM	6.6 [b] (7.4)[c]	

[a] calculated pK_a value by Šesták et al. [37].
[b] calculated pK_a value by Sladek et al. [57].
[c] experimentally measured pK_a values [58,59].

neutral form in accordance with known pK_a values of anilines. The pK_a values for the pyrrolidine nitrogen in all inhibitors were similar to the predicted and experimental values of natural products swainsonine and 1,4-dideoxy-1,4-imino-D-mannitol.

3. Conclusion

The series of 1,4-imino-L-lyxitols derivatives with a positively charged linker (amine, amidine and guanidine functions) were synthesized and tested their ability to inhibit α-mannosides from the GH family 38 of the fruit fly model system. The length of the charged linker correlated well with the measured IC_{50} values. The pyrrolidine **6** with the longest chain showed the best inhibitory properties. All tested 1,4-imino-L-lyxitols selectively bound to the target enzyme GMIIb with no significant inhibition of lysosomal α-mannosidases (models LManII and JBMan). These results further verified our previous study [37] that the stereo-configuration of multiple hydroxyl groups on the pyrrolidine ring tested as inhibitors in this and previous studies retains their selectivity properties toward Golgi α-mannosidase IIb, and it may be a lead structure in development of a selective inhibitor of human Golgi α-mannosidase II for an alternative treatment of cancer.

4. Experimental

4.1. General

TLC was performed on aluminium sheets pre-coated with silica gel 60 F254 (Merck). Visualization was achieved by immersing the plates into 10% solution of phosphomolybdic acid (PMA) in ethanol followed by heating the plate. Flash column chromatography was carried out on silica gel 60 (0.040–0.060 mm, Merck) with distilled solvents (hexanes, ethyl acetate, chloroform, methanol). All commercially available reagents and anhydrous solvents were used as received. All reactions containing sensitive reagents were carried out under an argon atmosphere. ^{1}H NMR and ^{13}C NMR spectra were recorded at 25 °C with the Bruker AVANCE III HD 400 and Bruker AVANCE III HDX 600 spectrometers. Chemical shifts are given in ppm (δ) relative to residual signal of appropriate deuterated solvent used ($CDCl_3$, CD_3OD). The ultrasonic bath USC-300TH was used for sonication. Optical rotations were determined on a Jasco P-2000 polarimeter at 20 °C.

High-resolution mass spectra were recorded with an Orbitrap Elite (Thermo Scientific) mass spectrometer with ESI ionization in positive mode.

4.2. General method for deprotection (Method A)

To a stirred solution of protected iminolyxitol in MeOH (3.5 mL / 0.1 mmol of iminolyxitol), 6 M HCl (1.75 mL, 6 M HCl : MeOH 1:2, v/v) was added while cooling in an ice-water bath. After 15 min., the ice water bath was removed and the stirring was continued at rt for 16 h. Then, HCl was carefully neutralized with solid Na_2CO_3 (1.5 eq. regarding HCl used). The resulting suspension was filtered, the filter cake was washed with MeOH (10 mL) and the filtrate was evaporated to dryness. The residue was again suspended in MeOH (30 mL), filtered and the filtrate was evaporated. The residue was purified by column chromatography ($CHCl_3$:MeOH + 0.5% (v/v) of concd. aqueous NH_3).

4.3. General method for deprotection (Method B)

To a stirred solution of protected iminolyxitol in MeOH (3.5 mL/ 0.1 mmol of iminolyxitol), 6 M HCl (1.75 mL, 6 M HCl : MeOH 1:2, v/v) was added while cooling in an ice-water bath. After 15 min., the ice water bath was removed and the stirring was continued at rt for 16 h. The solvent was evaporated. The residue was redissolved in water (10 mL) and washed with DCM (3 × 10 mL). Lyophilization of the water layer gave desired product as hydrochloride.

4.3.1. N-4-Aminomethylbenzyl-1,4-dideoxy-1,4-imino-L-lyxitol (5)

Deprotection of **4** (193 mg, 0.47 mmol) was carried out according to general procedure (Method A). Purification of the crude product by column chromatography ($CHCl_3$:MeOH 7:1 → 5:1 + 0.5% (v/v) of conc. aqueous NH_3) afforded **5** (93 mg, 78%). Yellowish oil, $[\alpha]_D^{20}$ + 17.1 (c 0.2, CH_3OH). ^{1}H NMR (400 MHz, CD_3OD): δ 7.36 (d, 2H, J = 8.1 Hz, Ar), 7.32 (d, 2H, J = 8.1 Hz, Ar), 4.26 (dd, 1H, J = 5.1, 7.1 Hz, H-3), 4.08 (td, 1H, J = 3.0, 5.2 Hz, H-2), 3.97 (d, 1H, J = 13.1 Hz, NCH_2Ph), 3.81 (s, 2H, CH_2NH$_2$), 3.73 (dd, 1H, J = 5.3, 11.1 Hz, H-5′), 3.66 (dd, 1H, J = 3.6, 11.1 Hz, H-5), 3.53 (d, 1H, J = 13.1 Hz, NCH_2Ph), 2.88 (dd, 1H, J = 3.0, 10.6 Hz, H-1′), 2.84 (ddd, 1H, J = 3.6, 5.2, 7.1 Hz, H-4), 2.56 (dd, 1H, J = 5.3, 10.6 Hz, H-1). ^{13}C NMR (100 MHz, CD_3OD): δ 142.3 (Ar), 138.7 (Ar), 130.4 (Ar), 128.4 (Ar), 73.7 (C-3), 71.5 (C-2), 67.6 (C-4), 60.9 (C-5), 60.0 (NCH_2Ph), 59.1 (C-1), 46.4 (CH_2NH_2). HRMS (ESI-MS): m/z: calcd for $[C_{13}H_{20}N_2O_3]H^+$: 253.1552, found: 253.1545.

4.3.2. 1,4-Dideoxy-N-4-guanidinomethylbenzyl-1,4-imino-L-lyxitol.HCl (6)

The compound **4** (117 mg, 0.25 mmol) was dissolved in mixture of THF/DMF (9 mL, 2:1, v/v) and *N*,*N*′-bis(*tert*-butoxycarbonyl)-1*H*-pyrazole-1-carboxamidine (86 mg, 0.28 mmol) was added. The mixture was sonicated at rt for 1 h. Then, the solvent was evaporated, the residue was redissolved in DCM (15 mL) and tris-(2-aminoethyl)amine polystyrene resin was added to scavenge the excess of *N*,*N*′-bis(*tert*-butoxycarbonyl)-1*H*-pyrazole-1-carboxamidine. The resulting suspension was stirred at rt for 5 days. The resin was filtered off and the solvent was removed. The crude product was deprotected according to general procedure (Method B) to give 6 as HCl salt (65 mg, 77% after 2 steps). Colorless oil, $[\alpha]_D^{20}$ + 10.4 (c 0.25, CH_3OH). ^{1}H NMR (400 MHz, CD_3OD): δ 7.62 (d, 2H, J = 8.1 Hz, Ar), 7.46 (d, 2H, J = 8.0 Hz, Ar), 4.70 (d, 1H, J = 12.9 Hz, NCH_2Ar), 4.48 (s, 2H, ArCH_2-guanidine), 4.42–4.35 (m, 3H, H-2, H-3, NCH_2Ar), 4.02 (dd, J = 8.0, 12.2 Hz, 1H, H-5′), 3.87 (dd, J = 4.2, 12.3 Hz, 1H, H-5), 3.80 (ddd, J = 3.6, 5.3, 7.2 Hz, 1H, H-4), 3.43 (dd, J = 5.5, 11.8 Hz, 1H, H-1′), 3.25 (dd, J = 5.0, 12.0 Hz, 1H, H-1). ^{13}C NMR (100 MHz, CD_3OD): δ 158.8 (NH−C(=NH)(NH$_2$)), 139.9 (Ar), 132.9 (Ar), 131.0 (Ar), 129.1 (Ar), 72.1 (C-3), 71.5 (C-4), 70.4 (C-2), 60.6 (NCH_2Ar), 59.4 (C-5), 57.0 (C-1), 45.4 (CH_2-NH-C(=NH)(NH$_2$)). HRMS (ESI-MS): m/z: calcd for $[C_{14}H_{22}N_4O_3]H^+$: 295.1770, found: 295.1765.

4.3.3. N-4-Amidinobenzyl-1,4-dideoxy-1,4-imino-L-lyxitol.HCl (9)

Deprotection of **8** (200 mg, 0.48 mmol) carried out according to general procedure (Method B) afforded **9** as hydrochloride (106 mg, 84%). Brown oil, $[\alpha]_D^{20}$ + 8.7 (c 0.25, CH_3OH). ^{1}H NMR (400 MHz, CD_3OD): δ 7.94 (d, 2H, J = 8.5 Hz, Ar), 7.88 (d, 2H, J = 8.5 Hz, Ar), 4.84 (d, 1H, J = 13.0 Hz, NCH_2Ar), 4.54 (d, 1H, J = 13.0 Hz, NCH_2Ph), 4.46–4.44 (m, 2H, H-2, H-3), 4.08 (dd, 1H, J = 8.2, 12.2 Hz, H-5′), 3.93 (dd, 1H, J = 4.2, 12.2 Hz, H-5), 3.90–3.85 (m, 1H, H-4), 3.48 (dd, 1H, J = 5.7, 12.3 Hz, H-1′), 3.31 (dd, 1H, J = 4.7, 12.3 Hz, H-1). ^{13}C NMR (100 MHz, CD_3OD): δ 167.8 (H_2N−C=NH), 137.4 (Ar), 133.3 (Ar), 131.0 (Ar), 129.8 (Ar), 72.1, 72.1, 70.5 (C-2, C-3, C-4), 60.2 (NCH_2Ph), 59.5 (C-5), 57.4 (C-1). HRMS (ESI-MS): m/z: calcd for $[C_{13}H_{19}N_3O_3]H^+$: 266.1504. Found: 266.1500.

4.3.4. N-4-(2-Aminoethyl)benzyl-1,4-dideoxy-1,4-imino-L-lyxitol (14)

Deprotection of **13** (101 mg, 0.24 mmol) was carried out according to general procedure (Method A). Purification of the crude product by column chromatography ($CHCl_3$:MeOH 1:0 → 5:1 + 0.5% v/v of conc. aqueous NH_3) afforded **14** (47 mg, 75%). Yellow oil, $[\alpha]_D^{20}$ + 27.2 (c 0.25, CH_3OH). ^{1}H NMR (600 MHz, CD_3OD): δ 7.32 (d, 2H, J = 7.9 Hz, Ar), 7.20 (d, 2H, J = 8.0 Hz, Ar), 4.26 (dd, 1H, J = 5.1, 7.1 Hz, H-3), 4.07 (td, 1H, J = 3.0, 5.2 Hz, H-2), 3.95 (d, 1H, J = 13.1 Hz, NCH_2Ar), 3.70 (dd, 1H, J = 5.4, 11.1 Hz, H-5′), 3.62 (dd, 1H, J = 3.5, 11.1 Hz, H-5), 3.50 (d, 1H, J = 13.1 Hz, NCH_2Ar), 2.92 (t, 2H, J = 7.3 Hz, CH_2CH$_2$NH$_2$), 2.87 (dd, 1H, J = 3.0, 10.6 Hz, H-1′), 2.83 (ddd, 1H, J = 3.6, 5.4, 7.2, Hz, H-4), 2.79 (t, 2H, J = 7.3 Hz, CH$_2$CH_2NH$_2$), 2.55 (dd, 1H, J = 5.2 10.6, Hz, H-1). ^{13}C NMR (150 MHz, CD_3OD): δ 139.4 (Ar), 138.0 (Ar), 130.5 (Ar), 129.7 (Ar), 73.7 (C-3), 71.5 (C-2), 67.7 (C-4), 60.8 (C-5), 60.0 (NCH_2Ar), 59.1 (C-1), 43.8 (CH_2CH$_2$NH$_2$), 38.9 (CH$_2$CH_2NH$_2$). HRMS (ESI-MS): m/z: calcd for $[C_{14}H_{22}N_2O_3]H^+$: 267.1703, found: 267.1703.

4.3.5. N-4-Aminobenzyl-1,4-dideoxy-1,4-imino-L-lyxitol (24)

Deprotection of **19** (109 mg, 0.28 mmol) was carried out according to general procedure (Method A). Purification of the crude product by column chromatography ($CHCl_3$:MeOH 7:1 → 5:1 + 0.5% v/v of conc. aqueous NH_3) gave **24** (54 mg, 82%). Yellowish oil, $[\alpha]_D^{20}$ - 25.7 (c 0.2, CH_3OH). ^{1}H NMR (400 MHz, CD_3OD): δ 7.22 (d, 2H, J = 8.4 Hz, Ar), 6.75 (d, 2H, J = 8.4 Hz, Ar), 4.32–4.22 (m, 3H, H-2, H-3, NCH_2Ar), 4.01 (d, 1H, J = 12.8 Hz, NCH_2Ar), 3.91 (dd, 1H, J = 6.7, 11.9 Hz, H-5′), 3.84 (dd, 1H, J = 4.8, 11.9 Hz, H-5), 3.48–3.46 (m, 1H, H-4), 3.16 (d, 2H, J = 5.2 Hz, H-1, H-1′). ^{13}C NMR (100 MHz, CD_3OD): δ 150.3 (Ar), 132.9 (Ar), 116.1 (Ar), 72.62 (C-3), 70.7 (C-2), 69.4 (C-4), 60.5 (NCH_2Ar), 59.7 (C-5), 57.0 (C-1). HRMS (ESI-MS): m/z: calcd for $[C_{12}H_{18}N_2O_3]H^+$: 239.1395, found: 239.1390.

4.3.6. N-3-Aminobenzyl-1,4-dideoxy-1,4-imino-L-lyxitol (25)

Deprotection of **21** (107 mg, 0.27 mmol) was carried out according to general procedure (Method A). The crude product was purified by column chromatography ($CHCl_3$:MeOH 7:1 → 5:1 + 0.5% v/v of conc. aqueous NH_3) to obtain **25** (56 mg, 87%). Yellowish oil, $[\alpha]_D^{20}$ + 5.1 (c 0.2, CH_3OH). ^{1}H NMR (600 MHz, CD_3OD): δ 7.07 (t, 1H, J = 7.7 Hz, Ar), 6.76 (s, 1H, Ar), 6.70 (d, 1H, J = 7.5 Hz, Ar), 6.65 (dd, 1H, J = 1.3, 7.9 Hz, Ar), 4.25 (dd, J = 5.2, 7.0 Hz, 1H, H-3), 4.07 (td, 1H, J = 3.2, 5.1 Hz, H-2), 3.87 (d, 1H, J = 13.0 Hz, NCH_2Ar), 3.73 (dd, 1H, J = 5.4, 11.1 Hz, H-5′), 3.66 (dd, 1H, J = 3.5, 11.1 Hz, H-5), 3.45 (d, 1H, J = 13.0 Hz, NCH_2Ar), 2.92 (dd, 1H, J = 2.9, 10.7 Hz, H-1′), 2.85 (ddd, 1H, J = 3.6, 5.3, 7.0 Hz, H-4), 2.59 (dd, 1H, J = 5.3, 10.7 Hz, H-1). ^{13}C NMR (150 MHz, CD_3OD): δ 148.6 (Ar), 140.4 (Ar), 129.9 (Ar), 120.3 (Ar), 117.5 (Ar), 115.6 (Ar), 73.7 (C-3), 71.5 (C-2), 67.6 (C-4), 60.7 (C-5), 60.4 (NCH_2Ar), 59.0 (C-1). HRMS (ESI-MS): m/z: calcd for $[C_{12}H_{18}N_2O_3]H^+$: 239.1396, found: 239.1392.

4.3.7. 1,4-Dideoxy-N-4-fluorobenzyl-1,4-imino-L-lyxitol (26)

Deprotection of **22** (195 mg, 0.49 mmol) was carried out according to general procedure (Method A). The crude product was purified by column chromatography ($CHCl_3$:MeOH 7:1 → 5:1 + 0.5% v/v of conc. aqueous NH_3) to give **26** (76 mg, 64%). Colorless oil, $[\alpha]_D^{20}$ + 71.4 (c 0.25, CH_3OH). ^1H NMR (400 MHz, CD_3OD) δ 7.42–7.38 (m, 2H, Ar), 7.09–7.03 (m, 2H, Ar), 4.28 (dd, 1H, J = 5.0, 7.1 Hz, H-3), 4.10 (td, 1H, J = 3.1, 5.1 Hz, H-2), 4.00 (d, 1H, J = 13.2 Hz, NCH_2Ar), 3.74 (dd, 1H, J = 5.2, 11.2 Hz, H-5′), 3.67 (dd, 1H, J = 3.7, 11.2 Hz, H-5), 3.55 (d, 1H, J = 13.2 Hz, NCH_2Ar), 2.92–2.84 (m, 2H, H-1′, H-4), 2.58 (dd, 1H, J = 5.2, 10.6 Hz, H-1). ^{13}C NMR (100 MHz, CD_3OD): δ 163.5 (d, J = 243.8 Hz, Ar), 135.7 (d, J = 3.2 Hz, Ar), 132.0 (d, J = 8.0 Hz, Ar), 115.9 (d, J = 21.5 Hz, Ar), 73.7 (C-3), 71.5 (C-2), 67.8 (C-4), 60.8 (C-5), 59.5 (NCH_2Ar), 58.5 (C-1). HRMS (ESI-MS): m/z: calcd for $[C_{12}H_{16}FNO_3]H^+$: 242.1187, found: 242.1186.

4.3.8. 1,4-Dideoxy-N-4-hydroxybenzyl-1,4-imino-L-lyxitol (27)

Deprotection of **23** (107 mg, 0.21 mmol) was carried out according to general procedure (Method A). The crude product was purified by column chromatography ($CHCl_3$:MeOH 1:0 → 5:1 + 0.5% v/v of conc. aqueous NH_3) to give **27** (35 mg, 70%). Colorless oil, $[\alpha]_D^{20}$ - 46.5 (c 0.25, CH_3OH). ^1H NMR (600 MHz, CD_3OD): δ 7.28 (d, 2H, J = 8.5 Hz, Ar), 6.82 (d, 2H, J = 8.6 Hz, Ar), 4.31 (dd, 1H, J = 4.6, 6.4 Hz, H-3), 4.26 (d, 1H, J = 13.0 Hz, NCH_2Ar), 4.22 (dt, 1H, J = 2.8, 6.4 Hz, H-2), 3.95 (d, 1H, J = 13.0 Hz, NCH_2Ar), 3.86 (dd, 1H, J = 6.2, 11.8 Hz, H-5′), 3.80 (dd, 1H, J = 4.7, 11.8 Hz, H-5), 3.38 (dd, 1H, J = 5.6, 10.6 Hz, H-4), 3.11 (dd, 1H, J = 4.6, 11.5 Hz, H-1′), 3.05 (dd, 1H, J = 5.5, 11.5 Hz, H-1). ^{13}C NMR (150 MHz, CD_3OD): δ 159.4 (Ar), 133.0 (Ar), 125.0 (Ar), 116.6 (Ar), 72.7 (C-3), 70.8 (C-2), 69.3 (C-4), 60.1 (NCH_2Ar), 59.8 (C-5), 57.4 (C-1). HRMS (ESI-MS): m/z: calcd for $[C_{12}H_{17}NO_4]H^+$: 240.1230, found: 240.1227.

4.4. Enzyme assays with class II α-Mannosidases (GH family 38)

The isolation and purification of recombinant *Drosophila melanogaster* Golgi (GMIIb) and lysosomal (LManII) α-mannosidases was carried out as already described [38]. The α-mannosidase from *Canavalia ensiformis* (Jack bean) (JBMan) was purchased from Sigma. The mannosidase activity of these enzyme preparations were measured using *p*-nitrophenyl-α-D-mannopyranoside (*p*NP-Man; Sigma; 100 mM stock in dimethylsulphoxide) as a substrate at the 2 mM final concentration in 50 mM acetate buffer at the relevant previously-defined optimal pH) (JBMan at pH 5.0, GMIIb at pH 6.0, and LManII at pH 5.2) and 0.5 μL of the enzyme (0.05 μg of protein for JBMan), in a total volume of 50 μL for 1–2 h at 37 °C. GMIIb was assayed in the presence of 0.5 mM $CoCl_2$.

The pyrrolidines **5**, **6**, **9**, **14**, **24–27** used in enzyme assays were lyophilized before the use. The inhibitors **5, 6, 9, 14, 24–27** were preincubated with the enzyme in the buffer for 5 min at rt and the reaction was started by addition of the substrate. The reactions were terminated with two volumes (0.1 mL) of 0.5 M sodium carbonate and the production of *p*-nitrophenol was measured at 405 nm using a multimode reader Mithras LB943 (Berthold Technologies). The average or representative result of three independent experiments made in duplicate is presented. The IC_{50} value was determined with 2 mM *p*NP-Man. The K_i values were determined from Dixon plots of assays performed with *p*NP-Man at the indicated concentration (0.5–4 mM).

4.5. Molecular modeling

Docking with Glide. The crystal structures of dGMII (PDB ID: 3BLB) [47,49], bLMan (PDB ID: 1O7D) [32] and homology model of GMIIb were used as 3-D enzyme models of human GMII for docking of synthesized pyrrolidines with the GLIDE program [60,61] of the Schrödinger package. Protonation states of amino acid residues of enzymes were calculated for the pH = 6.0 ± 1 (dGMII and GMIIb) and 4.5 ± 1 (bLMan) by the Protein Preparation Wizard of the Schrödinger package [62]. For docking with dGMII all molecules of water at the active site of dGMII were deleted except one (WAT1820, numbering according to PDB ID: 3BLB). This water has been shown to be conserved in crystal structures of dGMII either with intact substrates or inhibitors [40,47,50]. In all docking calculations the catalytic acid (Asp341 in case of dGMII, Asp431 in GMIIb and Asp319 in bLMan) was modelled in the protonated form in accordance with its catalytic role as a general acid. The receptor box for the docking conformational search was centered at the Zn^{2+} ion co-factor at the bottom of the active site with a size of 39 × 39 × 39 Å using partial atomic charges for the receptor from the OPLS2005 force field except for the Zn^{2+} and side chains of His90, Asp92, Asp204, Arg228, Tyr269, Asp341 and His471 (analogous residues were selected for GMIIb and bLMan). For these structural fragments the charges were calculated at the quantum mechanics level with the DFT (Density Functional Theory) method (M06-2X) [63] using a hybrid quantum mechanics/molecular mechanics (QM/MM) model (M06-2X/LACVP**:OPLS2005) with the QSite [64–66] program of the Schrödinger package. The grid maps were created with no Van der Waals radius and charge scaling for the atoms of the receptor. Flexible docking in standard (SP) precision was used. The partial charges of the ligands were calculated at the DFT level (M06-2X/LACVP**) using the Jaguar program [66] of the Schrödinger package. The potential for nonpolar parts of the ligands was softened by scaling the Van der Waals radii by a factor of 0.8 for atoms of the ligands with partial atomic charges less than specified cut-off of 0.15. The 5000 poses were kept per ligand for the initial docking stage with scoring window of 100 kcal mol^{-1} for keeping initial poses; the best 400 poses were kept per ligand for energy minimization. The ligand poses with RMS deviations less than 0.5 Å and maximum atomic displacement less than 1.3 Å were discarded as duplicates. The post-docking minimization for 10 ligand poses with the best docking score was performed and optimized structures were saved for subsequent analyses using the MAESTRO [67] viewer of the Schrödinger package.

Homology modeling. A 3-D model of GMIIb based on a sequence (UniProtKB – O97043) was built using the Modeller9v2 program [68].

pK_a calculations. The pK_a values of ligands in water were calculated at the quantum mechanics level including empirical corrections from the pK_a prediction module [69] of the Jaguar program [66] of the Schrödinger package.

Acknowledgement

This work was supported by the Slovak Research and Development Agency, Slovakia (the project APVV-0484-12), Scientific Grant Agency of the Ministry of Education of Slovak Republic and Slovak Academy of Sciences, Slovakia (the project VEGA-2/0064/15) and the Research & Development Operational Programme funded by the ERDF, EU. (Amplification of the Centre of Excellence on Green Chemistry Methods and Processes, CEGreenII, Contract No. 26240120025).

Appendix A. Supplementary material

Experimental details (synthesis of the intermediates 4, 7, 8, 10–13, 16–23), 1H and ^{13}C NMR spectra of the target pyrrolidines 5, 6, 9, 14, 24–27 and IC50 plots for the inhibition experiments towards GMIIb from Drosophila melanogaster for 5, 6, 9, 14, 24–27 and Dixon plots for the inhibition of GMIIb by compound 6. Coordinates of complexes of the docked inhibitors with dGMII (PDB ID: 3BLB) and GMIIb (homology models). Supplementary data to this article can be found online at https://doi.org/10.1016/j.bioorg.2018.10.066.

References

[1] P. Compain, O. Martin, Iminosugars: From Synthesis toTherapeutic Applications, Wiley, 2007.
[2] N. Asano, Curr. Top. Med. Chem. 3 (2003) 471–484.

[3] A. Varki, Cell 126 (2006) 841–845.
[4] T.M. Wrodnigg, A.J. Steiner, B.J. Ueberbacher, Anti-Cancer Agents Med. Chem. 8 (2008) 77–85.
[5] D.S. Alonzi, K.A. Scott, R.A. Dwerk, N. Zizmann, Biochem. Soc. Trans. 45 (2017) 571–582.
[6] K.L. Warfield, D.L. Barnard, S.G. Enterlein, D.F. Smee, M. Khaliq, A. Sampath, M.V. Callahan, U. Ramstedt, C.W. Day, Viruses 8 (2016) 71.
[7] J. Chang, T.K. Warren, X. Zhao, T. Gill, F. Guo, L. Wang, M.A. Comunale, Y. Du, D.S. Alonzi, W. Yu, H. Ye, F. Liu, J.-T. Guo, A. Mehta, A. Cocunati, T.S. Butters, S. Bavari, X. Xu, T.M. Block, Antiviral Res. 98 (2013) 432–440.
[8] A. Vasella, G.J. Davies, M. Bohm, Curr. Opin. Chem. Biol. 6 (2002) 619–629.
[9] A.E. Stütz, T.M. Wrodnigg, Adv. Carbohydr. Chem. Biochem. 66 (2011) 187–298.
[10] C. Parmeggiani, S. Catarzi, C. Matassini, G. D'Adamio, A. Morrone, A. Goti, P. Paoli, F. Cardona, ChemBioChem 16 (2015) 2054–2064.
[11] I.-J. Kang, S.-J. Hsu, H.-Y. Yang, T.-K. Yeh, C.-C. Lee, Y.-C. Lee, Y.-W. Tian, J.-S. Song, T.-A. Hsu, Y.-S. Chao, A. Yueh, J.-H. Chern, J. Med. Chem. 60 (2017) 228–247.
[12] V.K. Harit, N.G. Ramesh, RSC Adv. 6 (2016) 109528–109607.
[13] T.J.R. Cheng, T.H. Chan, E.L. Tsou, S.Y. Chang, W.Y. Yun, P.J. Yang, Y.T. Wu, W.C. Cheng, Chem. Asian. J. 8 (2013) 2600–2604.
[14] J. Calveras, M. Egido-Gabás, L. Gómez, J. Casas, T. Parella, J. Joglar, J. Bujons, P. Clapés, Chem. Eur. J. 15 (2009) 7310–7328.
[15] T.M. Chapman, S. Courtney, P. Hay, B.G. Davis, Chem. Eur. J. 9 (2003) 3397–3414.
[16] J.H. Kim, M.J. Curtis-Long, W.D. Seo, J.H. Lee, B.W. Lee, Y.J. Yoon, K.Y. Kang, K.H. Park, Bioorg. Med. Chem. Lett. 15 (2005) 4282–4285.
[17] A. Kato, Z.-L. Zhang, H.-Y. Wang, Y.-M. Jia, C.-Y. Yu, K. Kinami, Y. Hirokami, Y. Tsuji, I. Adachi, R.J. Nash, G.W.J. Fleet, J. Koseki, I. Nakagome, S. Hirono, J. Org. Chem. 80 (2015) 4501–4515.
[18] A. Kato, I. Nakagome, K. Sato, A. Yamamoto, I. Adachi, R.J. Nash, G.W.J. Fleet, Y. Natori, Y. Watanabe, T. Imahori, Y. Yoshimura, H. Takahata, S. Hirono, Org. Biomol. Chem. 14 (2016) 1039–1048.
[19] M. Martínez-Bailén, A.T. Carmona, E. Moreno-Claviko, I. Robina, D. Ide, A. Kato, A.J. Moreno-Vargas, Euro. J. Med. Chem. 138 (2017) 532–542.
[20] S.M. Colegate, P.R. Dorling, C.R. Huxtable, Aust. J. Chem. 32 (1979) 2257–2264.
[21] M. Bols, O. Lopez, F. Ortega-Caballero, Glycosidase inhibitors: structure, activity, synthesis, and medical relevance. In: J.P. Kamerling (Ed.), Comprehensive Glycoscience, Elsevier, Oxford, vol. 1, 2007, pp. 815–884.
[22] G. Legler, Glycosidase inhibition by basic sugar analogs and the transition state of enzymatic glycoside hydrolysis, in: A.E. Stütz (Ed.), Inimosugars as Glycosidase Inhibitors: Nojirimycin and beyond, Wiley-VCH Verlag GmbH, Weinheim, 1999, pp. 31–67.
[23] P.E. Goss, M.A. Baker, J.P. Carver, J.W. Dennis, Clin. Cancer Res. 1 (1995) 935–944.
[24] D.R. Rose, Curr. Opin. Struct. Biol. 22 (2012) 558–562.
[25] D.R.P. Tulsiani, O. Touster, Arch. Biochem. Biophys. 224 (1983) 594–600.
[26] D.R.P. Tulsiani, O. Touster, J. Biol. Chem. 258 (1983) 7578–7585.
[27] J.W. Dennis, K. Koch, S. Yousefi, I. Vanderelst, Cancer Res. 50 (1990) 1867–1872.
[28] K. Olden, P. Breton, K. Grzegorzewski, Y. Yasuda, B.L. Gause, O.A. Oredipe, S.A. Newton, S.L. White, Pharmacol. Ther. 50 (1991) 285–290.
[29] P.E. Goss, C.L. Reid, D. Bailey, J.W. Dennis, Clin. Cancer Res. 3 (1997) 1077–1086.
[30] P.E. Goss, J. Baptiste, B. Fernandes, M. Baker, J.W. Dennis, Cancer Res. 54 (1994) 1450–1457.
[31] Y.F. Liao, A. Lal, K.W. Moremen, J. Biol. Chem. 271 (1996) 28348–28358.
[32] P. Heikinheimo, R. Helland, H.K.S. Leiros, I. Leiros, S. Karlsen, G. Evjen, R. Ravelli, G. Schoehn, R. Ruigrok, O.-K. Tollesrud, S. McSweeney, E. Hou, J. Mol. Biol. 327 (2003) 631–644.
[33] P.M. Novikoff, O. Touster, A.B. Novikoff, D.P. Tulsiani, J. Cell Biol. 101 (1985) 339–349.
[34] M. Poláková, S. Šesták, E. Lattová, L. Petruš, J. Mucha, I. Tvaroška, J. Kóňa, Eur. J. Med. Chem. 46 (2011) 944–952.
[35] M. Poláková, R. Stanton, I.B.H. Wilson, I. Holková, S. Šesták, E. Machová, Z. Jandová, J. Kóňa, Carbohydr. Res. 406 (2015) 34–40.
[36] M. Poláková, R. Horák, S. Šesták, I. Holková, Carbohydr. Res. 428 (2016) 62–71.
[37] S. Šesták, M. Bella, T. Klunda, S. Gurská, P. Džubák, F. Wols, I.B.H. Wilson, V. Sladek, M. Hajdúch, M. Poláková, J. Kóňa, ChemMedChem 13 (2018) 373–383.
[38] I. Nemčovičová, S. Šesták, D. Rendić, M. Plšková, J. Mucha, I.B.H. Wilson, Glycoconjugate J. 30 (2013) 899–909.
[39] J.M.H. van den Elsen, D.A. Kuntz, D.R. Rose, EMBO J. 20 (2001) 3008–3017.
[40] N. Shah, D.A. Kuntz, D.R. Rose, Proc. Natl. Acad. Sci. USA 105 (2008) 9570–9575.
[41] A. Goeminne, M. McNaughton, G. Bal, G. Surpateanu, P. Van Der Veken, S. De Prol, W. Versées, J. Steyaert, A. Haemers, K. Augustyns, Eur. J. Med. Chem. 43 (2008) 315–326.
[42] ABBOTT GMBH and CO. KG Patent: WO2006/40179 A1, 2006; Location in patent: Page/Page column 123; WO 2006/040179 A1.
[43] J. Liu, S. Krajangsri, T. Singh, G. De Seriis, N. Chumnanvej, H. Wu, P.G. Andersson, J. Am. Chem. Soc. 139 (2017) 14470–14475.
[44] Z.R. Cai, S.Y. Jabri, H. Jin, R.A. Lansdown, S.E. Metobo, M.R. Mish, R.M. Pastor, US2008/58315, 2008.
[45] D.V. Jarikote, C. ÓReilly, P.V. Murphy, Tetrahedron Lett. 51 (2010) 6776–6778.
[46] B.S.G. Kumar, G. Pohlentz, M. Schulte, M. Mormann, N.S. Kumar, Glycobiology 24 (2014) 252–261.
[47] D.A. Kuntz, S. Nakayama, K. Shea, H. Hori, Y. Uto, H. Nagasawa, D.R. Rose, ChemBioChem 11 (2010) 673–680.
[48] H. Fiaux, D.A. Kuntz, D. Hoffman, R.C. Janzer, S. Gerber-Lemaire, D.R. Rose, L. Juillerat-Jeanneret, Bioorg. Med. Chem. 16 (2008) 7337–7346.
[49] D.A. Kuntz, D.R. Rose, Golgi Mannosidase II in complex with swainsonine at 1.3 Angstrom, The Research Collaboratory for Structural Bioinformatics (RCSB): RCSB-Rutgers, RCSB-San Diego Supercomputer Center, and University of Wisconsin-Madison, http://www.rcsb.org. (accessed June 04, 2012; PDB ID: 3BLB).
[50] D.A. Kuntz, W. Zhong, J. Guo, D.R. Rose, G.J. Boons, ChemBioChem 10 (2009) 268–277.
[51] N.S. Kumar, D.A. Kuntz, X. Wen, B.M. Pinto, D.R. Rose, Proteins 71 (2008) 1484–1496.
[52] P. Englebienne, H. Fiaux, D.A. Kuntz, C.R. Corbeil, S. Gerber-Lemaire, D.R. Rose, N. Moitessier, Proteins 69 (2007) 160–176.
[53] S.P. Kawatkar, D.A. Kuntz, R.J. Woods, D.R. Rose, G.J. Boons, J. Am. Chem. Soc. 128 (2006) 8310–8319.
[54] D.A. Kuntz, A. Ghavami, B.D. Johnston, B.M. Pinto, D.R. Rose, Tetrahedron-Asymmetry 16 (2005) 25–32.
[55] L.M. Kavlekar, D.A. Kuntz, X. Wen, B.D. Johnston, B. Svensson, D.R. Rose, B.M. Pinto, Tetrahedron-Asymmetry 16 (2005) 1035–1046.
[56] O. Lopez, F.L. Qing, C.M. Pedersen, M. Bols, Bioorg. Med. Chem. 21 (2013) 4755–4761.
[57] V. Sladek, J. Kóňa, H. Tokiwa, Phys. Chem. Chem. Phys. 19 (2017) 12527–12537.
[58] P.R. Dorling, C.R. Huxtable, S.M. Colegate, Biochem. J. 191 (1980) 649–651.
[59] I.C. Dibello, G. Fleet, S.K. Namgoong, K. Tadano, B. Winchester, Biochem. J. 259 (1989) 855–861.
[60] T.A. Halgren, R.B. Murphy, R.A. Friesner, H.S. Beard, L.L. Frye, W.T. Pollard, J.L. Banks, J. Med. Chem. 47 (2004) 1750–1759.
[61] Glide, version 7.0, Schrödinger, LLC, New York, NY, 2016.
[62] Schrödinger Suite 2016 Protein Preparation Wizard, Epik v. 3.5, Impact v. 7.0, Schrödinger, Maestro v.10.5, LLC, New York, NY, 2016.
[63] Y. Zhao, D.G. Truhlar, Theor. Chem. Res. 120 (2008) 215–241.
[64] R.B. Murphy, D.M. Philipp, R.A. Friesner, J. Comput. Chem. 21 (2000) 1442–1457.
[65] Qsite, Schrödinger, LLC, New York, NY, 2016.
[66] Jaguar, version 9.1, Schrödinger, LLC, New York, NY, 2016.
[67] Maestro, version 10.5, Schrödinger, LLC, New York, NY, 2016. New York, NY, 2016.
[68] A. Sali, T.L. Blundell, J. Mol. Biol. 234 (1993) 779–815.
[69] J.J. Klicic, R.A. Friesner, S.Y. Liu, W.C. Guida, J. Phys. Chem. A 106 (2002) 1327–2133.